Characteristics of Iron Phosphate and Its Catalytic Activity for Oxidative Dehydrogenation of Isobutyric Acid

Etsuhiro Muneyama, Atsuhiro Kunishige, Kyoji Ohdan,† and Mamoru Ai*,††

UBE Scientific Analysis Laboratory, Inc., 1978-5 Kogushi, Ube 755

†Ube Laboratory, UBE Industries, Ltd., 1978-5 Kogushi, Ube 755

††Department of Applied Chemistry and Biotechnology, Niigata Institute of Technology,
1719 Fujihashi, Kashiwazaki 945-11

(Received August 29, 1995)

In the absence of oxygen, P/Fe = 1.2 catalyst samples are reduced by hydrogen or isobutyric acid to form $Fe_2P_2O_7$ via $Fe_3(P_2O_7)_2$, while the P/Fe = 1.0 samples are reduced directly to $Fe_2P_2O_7$; without passing through $Fe_3(P_2O_7)_2$. $Fe_2P_2O_7$ is oxidized by air to an unknown compound (Y-phase), but not to $Fe_3(P_2O_7)_2$ nor $FePO_4$. The Y-phase is reduced to $Fe_2P_2O_7$. During the use in the oxidative dehydrogenation of isobutyric acid, freshly calcined catalysts are reduced to $Fe_3(P_2O_7)_2$, while the $Fe_2P_2O_7$ catalysts are oxidized to Y-phase, though the rates are very slow. The catalytic activity and selectivity are scarcely affected by variation in the structure of the iron phosphate catalyst and in the oxidation states of iron ions. The P/Fe and $Fe^{2+}/(Fe^{2+}+Fe^{3+})$ ratios on the surface, which were measured from cooled catalyst samples, are almost the same as those in the bulk.

Iron phosphates are known in patents to be effective as catalysts for oxidative dehydrogenation of isobutyric acid (IBA) to methacrylic acid (MAA) similarly to heteropoly compounds based on 12-molybdophosphoric acid [$H_3PMo_{12}O_{40}$]. Indeed, there have been a number of scientific studies concerning the catalytic action of iron phosphate. As the structures of iron phosphates with a P/Fe atomic ratio of unity, quartz-type $FePO_4$ [$FePO_4$(Q)],1) tridymite-type $FePO_4$ [$FePO_4$(T)],2) and $Fe_2P_2O_7$3,4) are known. $Fe_2P_2O_7$ is generally obtained by reduction of $FePO_4$. Millet et al.5) reported the presence of a new phase containing both Fe^{2+} and Fe^{3+}, which was proposed to be $Fe_3(P_2O_7)_2$ [$Fe_4(P_2O_7)_3$+$Fe_2P_2O_7$; P/Fe = 1.33, $Fe^{2+}/(Fe^{2+}+Fe^{3+}) = 0.33$] having characteristic peaks in the X-ray powder pattern at $2\theta = 29.53°$ and 29.72°, and which was proposed to be associated with the catalytic action. According to the single crystal study by Ijjaali et al.,6) the X-ray diffraction (XRD) pattern of $Fe_3(P_2O_7)_2$ has peaks at $2\theta = 14.48°$, 21.14°, 21.26°, 24.84°, 34.86°, and 35.69°. On the other hand, Barbaux et al.7) reported that the presence of pyrophosphate groups such as $Fe_3(P_2O_7)_2$ is not proved.

It was found in our previous works8) that the structure of freshly prepared iron phosphates with a P/Fe atomic ratio close to unity varies with a rise in the calcination temperature as follows: amorphous $\xrightarrow{500\ °C}$ unidentified phase $\xrightarrow{550\ °C}$ $FePO_4$(Q) phase. This unidentified phase was later assigned to a $FePO_4$(T) phase, which has three main peaks in the XRD spectra at $2\theta = 20.00°$, 20.95°, and 29.35°.2) The excess of phosphorus with respect to the stoichiometry of $FePO_4$ or $Fe_2P_2O_7$, viz., P/Fe = 1.0, forms $NH_4FeP_2O_7 \cdot 1.5H_2O$ when the iron phosphate is prepared in the presence of ammonium ions, and this compound is transformed with a rise in the calcination temperature as follows: $NH_4FeP_2O_7 \cdot 1.5H_2O \xrightarrow{450\ °C} NH_4FeP_2O_7 \xrightarrow{500—550\ °C} FePO_4(Q) + NH_3 +$ polycondensed phosphates. It was proposed that species with a P/Fe ratio of unity are responsible for the catalytic action and that the compounds with a P/Fe ratio of more than unity such as $NH_4FeP_2O_7$, $FeH_2P_2O_7$, and polycondensed phosphates do not have the catalytic action.

It was also found9) that the catalytic actions such as activity and selectivity are scarcely affected with a large variation in the valence states of iron ions in the bulk.

In this study, to get more insight into the catalytic actions of iron phosphate, we attempted to clarify the variation in the structure, the oxidation states of iron ions both in the bulk and on the surface, and the P/Fe composition on the surface owing to the reduction and reoxidation and also to the use in the reaction.

Experimental

1. Catalysts. Iron Phosphate catalysts with P/Fe atomic ratios of 1.02, 1.2 and 1.33 were prepared by the "Method C" procedures described in our previous study.8) Unless otherwise indicated, the studies were done with the catalyst with a P/Fe ratio of 1.2. The surface area measured by the BET method was 15 $m^2\,g^{-1}$.

2. Characterizations. X-Ray powder diffraction patterns were studied using a Rigaku-Denki model RAD-RB diffractometer with Cu $K\alpha$ radiation.

The amounts of Fe^{2+} and Fe^{3+} ions in the bulk were measured by the redox titration method.10) The detailed procedures were described in a previous paper.11)

X-Ray photoelectron spectroscopy (XPS) analysis was done on an VG Escalab 200X photoelectron spectrometer with a hemispherical electrostatic analyzer. A Mg anode (1253.6 eV) was used. The instrumental resolution for the Au $4f_{7/2}$ signal was 1.2 eV. A titanum sublimation pump and ion pump gave a vacuum of 10^{-7} to 10^{-8} Pa. A powdered sample was mounted onto a sample holder made of nickel. All binding energies were referenced to contaminant carbon (C 1s = 284.6 eV).

The P/Fe atomic ratios were calculated based on the peak areas of phosphorus and Fe 2p, the Scofield photoionization cross sections, the mean free paths of the electrons, and the instrumental function, which was given by the ESCA manufacturer. Since Fe 2p spectrum has a intense background even on the high binding energy side, the content of iron on the surface is inevitably underestimated, if the background of Fe 2p is subtracted in the usual way for the calculation of Fe 2p areas.[12,13] Indeed, it is not easy to establish a true base line for the Fe 2p spectrum. To resolve this problem, we adopted the values of photoionization cross section of Fe 2p electrons, which were measured from commercially obtained $Fe_2P_2O_7$ and $FePO_4$ as standard compounds with a P/Fe ratio of unity.

The amounts of Fe^{2+} and Fe^{3+} on the surface were measured by Factor analysis of Fe 2p peaks using Fe^{2+} and Fe^{3+} spectra obtained from measurements for $Fe_2P_2O_7$ and $FePO_4$.[14]

3. Reaction Procedures. The vapor phase oxidation of IBA was done with a continuous-flow system at atmospheric pressure. The detailed procedures and definitions were the same as those described in our previous works.[11,15] Unless otherwise indicated, the reaction temperature was 400 °C and the feed rates of IBA, oxygen, water, and nitrogen were 21.5, 16.5, 324, and 350 mmol h^{-1}, respectively.

Results and Discussion

1. Reduction of Iron Phosphate. The freshly prepared iron phosphate samples were reduced at 400 °C in a stream of gaseous mixture of IBA, water, and nitrogen. The feed rates were 21.5, 324, and 350 mmol h^{-1}, respectively. The XRD spectra of the samples and the extents of reduction in the bulk, that is, the $Fe^{2+}/(Fe^{2+}+Fe^{3+})$ ratios, obtained at different times-on-stream are shown in Fig. 1.

The freshly prepared iron phosphate contains both $FePO_4$(Q) and $FePO_4$(T) with a small amount of $NH_4FeP_2O_7$ [Fig. 1 (A)]. It is reduced to $Fe_2P_2O_7$ via a bluish black intermediate compound with peaks in the XRD spectra at $2\theta = 19.96°$, 21.24°, 24.68°, 35.04°, 35.54°, 50.68°, and 63.12° [Fig. 1 (B—E)]. According to the studies by Ijjaali et al.,[6] this compound was assigned to $Fe_3(P_2O_7)_2$.

In the reduction of iron phosphates with a P/Fe ratio of 1.02, $Fe_2P_2O_7$ was obtained as the product, but $Fe_3(P_2O_7)_2$ was not observed as the intermediate compound. These findings suggest that the presence of excess phosphorus with respect to the stoichiometry of $FePO_4$ (P/Fe = 1.0) is required to form $Fe_3(P_2O_7)_2$ (P/Fe = 1.33) from $FePO_4$.

2. Oxidation of $Fe_2P_2O_7$. $Fe_2P_2O_7$ samples with a $Fe^{2+}/(Fe^{2+}+Fe^{3+})$ ratio of about 0.9 were prepared by reduction of the freshly calcined iron phosphate samples in a stream of hydrogen at 480 °C for 12 h. Then, the $Fe_2P_2O_7$ samples were reoxidized by passing a mixture of air and water at 400 °C. As the time-on-stream was increased, the $Fe^{2+}/(Fe^{2+}+Fe^{3+})$ ratio decreased gradually to about 0.22. The color of samples changed from white to dark red-brown.

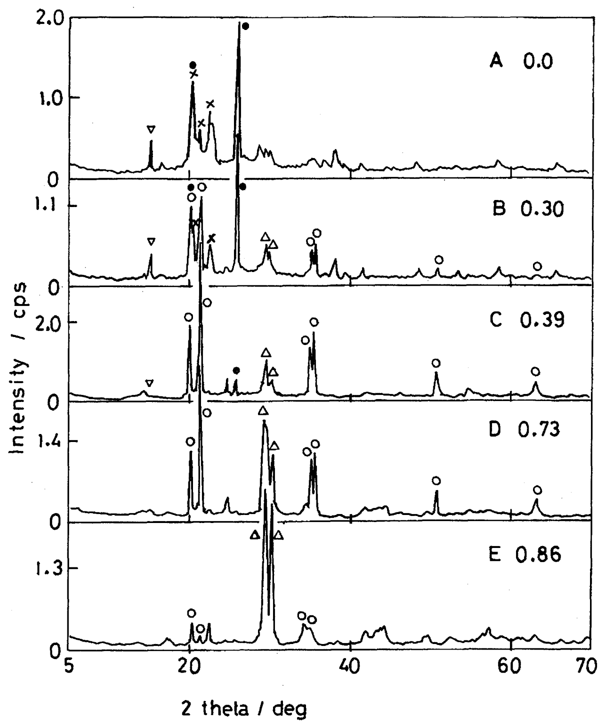

Fig. 1. XRD patterns of iron phosphates reduced by IBA. Reduction time (min): (A) 0; (B) 15; (C) 20; (D) 60; (E) 480. Figures denote the $Fe^{2+}/(Fe^{2+}+Fe^{3+})$ ratios. (●) $FePO_4$(Q); (×) $FePO_4$(T); (○) $Fe_3(P_2O_7)_2$; (△) $Fe_2P_2O_7$; (▽) $NH_4FeP_2O_7$.

Figure 2 shows the XRD spectra and the extent of reduction obtained at different times-on-stream. The $Fe_2P_2O_7$ phase is transformed to a new phase the XRD patterns of which had only one clear peak at $2\theta = 29.5°$. This phase is designated the Y-phase. It is concluded that the $Fe_2P_2O_7$ phase is oxidized to Y-phase, but not to $FePO_4$ nor $Fe_3(P_2O_7)_2$ under the conditions used. Y-phase was transformed slowly to $FePO_4$(Q) at about 1000 °C.

3. Reduction of Y-Phase. Iron phosphate samples consisting of Y-phase, which had previously been prepared by reoxidation of samples consisting of $Fe_2P_2O_7$ phase, was reduced again by passing the gaseous mixture of IBA, water, and nitrogen at 400 °C. It was found that the Y-phase is reduced to form a $Fe_2P_2O_7$ phase similarly to the freshly calcined sample consisting of $FePO_4$. It is clear that the transformation between $Fe_2P_2O_7$ and Y-phase is reversible.

4. Oxidation and Reduction of Iron Phosphate Containing $Fe_3(P_2O_7)_2$. Freshly calcined iron phosphate samples were reduced in a stream of the mixture of IBA, water, and nitrogen at 400 °C for 35 min. As may be seen in Fig. 3 (A), the resulting sample contains mainly $Fe_3(P_2O_7)_2$ and $Fe_2P_2O_7$. The same sample was then oxidized by air at 480 °C for 4 h. The XRD spectra shown in Fig. 3 (B) indicate that the $Fe_2P_2O_7$ phase is transformed to Y-phase, but that the $Fe_3(P_2O_7)_2$ phase remains unchanged. On the other hand, the samples consisting of $FePO_4$ and $Fe_3(P_2O_7)_2$ were obtained by the reduction for a shorter time (for less than 20 min). They were also oxidized by air. It was found that no clear change is observed in the XRD spectra upon the oxi-

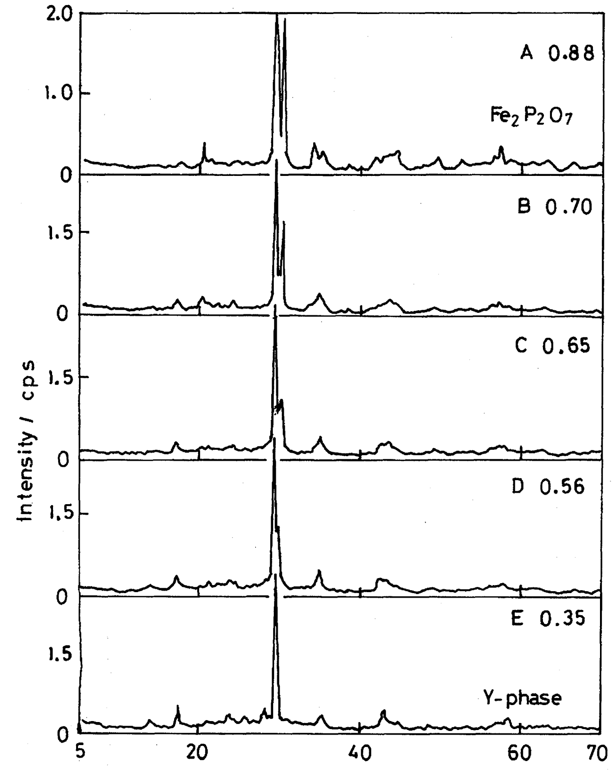

Fig. 2. XRD patterns of samples obtained by oxidation of $Fe_2P_2O_7$ at 400 °C. Oxidation time (min): (A) 0; (B) 30; (C) 120; (D) 240; (E) 240 (at 480 °C). Figures denote the $Fe^{2+}/(Fe^{2+}+Fe^{3+})$ ratios.

dation procedures, though the samples are clearly oxidized; the $Fe^{2+}/(Fe^{2+}+Fe^{3+})$ ratio decreased from 0.30 to 0.02.

The sample consisting of both $Fe_3(P_2O_7)_2$ and Y-phases [Fig. 3 (B)] was reduced in a stream of the mixture of IBA, water, and nitrogen at 400 °C for 25 min. The XRD spectra of the resulting samples are shown in Fig. 3 (C). It was found that the Y-phase was transformed to $Fe_2P_2O_7$, but that the $Fe_3(P_2O_7)_2$ phase remained unchanged.

We concluded from these findings that $Fe_3(P_2O_7)_2$ is formed irreversibly from $FePO_4$ and furthermore that it is markedly less oxidizable than $Fe_2P_2O_7$ and markedly less reducible than the Y-phase.

5. Variation in the Structure and Valence State by Use in the Oxidation of IBA. The reaction was done at 400 °C over freshly calcined iron phosphate samples. After 25 h of use in the reaction, the $Fe^{2+}/(Fe^{2+}+Fe^{3+})$ ratio increased from zero to 0.40. Only $Fe_3(P_2O_7)_2$ phase and a small amount of $FePO_4$ phase were observed in the XRD spectra. It is concluded that during the use in the oxidation reaction, the iron phosphate of the $FePO_4$ phase is reduced to $Fe_3(P_2O_7)_2$, but not to $Fe_2P_2O_7$ nor to Y-phase.

On the other hand, the reaction was also done at 400 °C over iron phosphate samples consisting of $Fe_2P_2O_7$. After 32 h of use in the reaction, the $Fe^{2+}/(Fe^{2+}+Fe^{3+})$ ratio decreased from 0.88 to 0.73. The XRD spectra showed that a part of $Fe_2P_2O_7$ phase was transformed to Y-phase, but the presence of $Fe_3(P_2O_7)_2$ and $FePO_4$ was not observed. It was therefore concluded that during the use in the reaction, a part of $Fe_2P_2O_7$ phase was reoxidized to Y-phase, but not to $FePO_4$ nor to $Fe_3(P_2O_7)_2$.

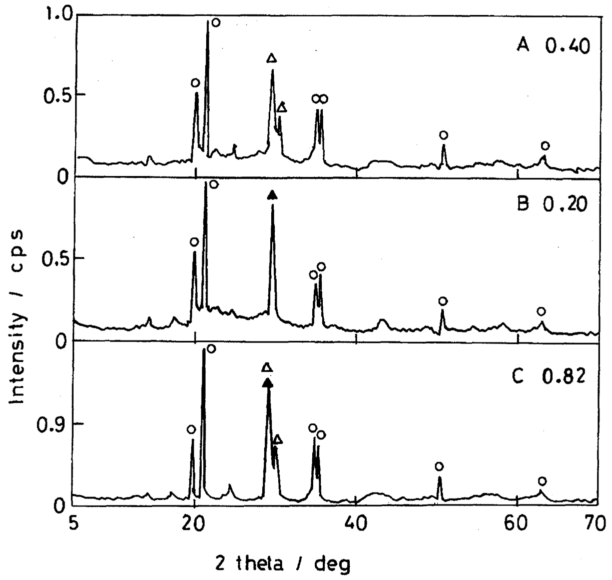

Fig. 3. Change in the XRD patterns due to the reduction and reoxidation. (A) sample obtained by partial reduction of a freshly prepared iron phosphate; (B) sample obtained by reoxidation of (A); (C) sample obtained by re-reduction of (B). Figures denote the $Fe^{2+}/(Fe^{2+}+Fe^{3+})$ ratios. (○) $Fe_3(P_2O_7)_2$; (△) $Fe_2P_2O_7$; (▲) Y-phase.

Then, the reaction was done over iron phosphate samples consisting mainly of Y-phase [$Fe^{2+}/(Fe^{2+}+Fe^{3+}) = 0.23$]. The samples were reduced much more rapidly than the samples consisting of $FePO_4$ and/or $Fe_3(P_2O_7)_2$ phase. The XRD spectra showed that a part of Y-phase was reduced to form $Fe_2P_2O_7$. This indicates that the transformation between $Fe_2P_2O_7$ and Y-phase takes place reversibly during use in the oxidation.

6. Effects of Variation in the Valence States of and Structure on the Catalytic Performance. The catalytic performances of iron phosphates that were different in both valence states and structures were measured under the fixed reaction conditions described in the Experimental section. The results are summarized in Table 1. It is clear that both the activity and selectivity are scarcely affected by a large variation in both valence states of iron ions and structures in the bulk in conformity with the previous results.[9]

7. XPS Studies. As mentioned above, the catalytic actions were found to be scarcely affected with a variation in the properties of bulk. This led us to study the properties on the surface by XPS, to get information to explain the catalytic actions.

The P/Fe atomic ratios on the surface were measured by XPS for freshly calcined iron phosphate samples that were different in the P/Fe ration in the bulk. The results are summarized in Table 2. It is clear that the P/Fe ratios on the surface are almost the same as those in the bulk. This means that no segregation of iron or phosphorus occurs between

Table 1. Catalytic Performances of Iron Phosphates

Phase observed in XRD spectra		$\frac{Fe^{2+}}{Fe^{2+}+Fe^{3+}}$	Conversion of IBA	Selectivity to MAA
Main	Minor		%	mol%
$FePO_4$(Q)	$FePO_4$(T)	0.0—0.1	86.2	78.5
			92.6	77.0
$Fe_3(P_2O_7)_2$	$FePO_4$(Q)	0.4	84.10	82.0
Y-phase	—	0.4—0.6	83.0	82.5
			85.0	81.0
$Fe_2P_2O_7$	Y-phase	0.7—0.8	85.0	82.5
			89.0	82.0
$Fe_2P_2O_7$	—	0.9—0.95	79.0	82.0
			85.0	80.5

Reaction temperature, 400 °C; contact time, 0.4 s; feed rates of IBA/oxygen/water/nitrogen = 21.5/16.5/324/350 mmol h^{-1}. The results were obtained after about 2 to 3 h from the start.

Table 2. P/Fe Composition on the Surface of Freshly Prepared Iron Phosphates

Nominal (Bulk)	XPS (Surface)
1.0	1.05
1.2	1.16
1.5	1.52

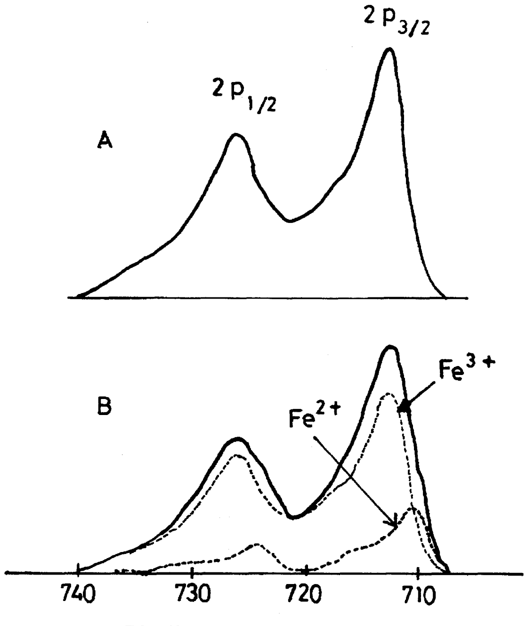

Fig. 4. XPS spectra for Fe 2p of iron phosphate catalysts. (A) fresh catalyst; (B) used catalyst. Dashed lines: Fe^{2+} and Fe^{3+} obtained by peak resolving.

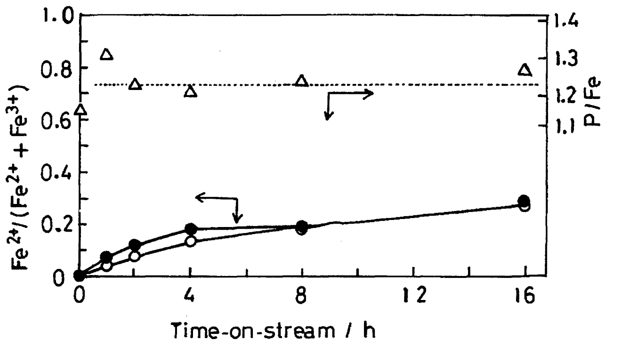

Fig. 5. Variation in P/Fe and $Fe^{2+}/(Fe^{2+}+Fe^{3+})$ ratios as a function of the time of IBA oxidation. (○) in the bulk; (●) on the surface. Sample: freshly prepared iron phosphate. Reaction temperature: 380 °C.

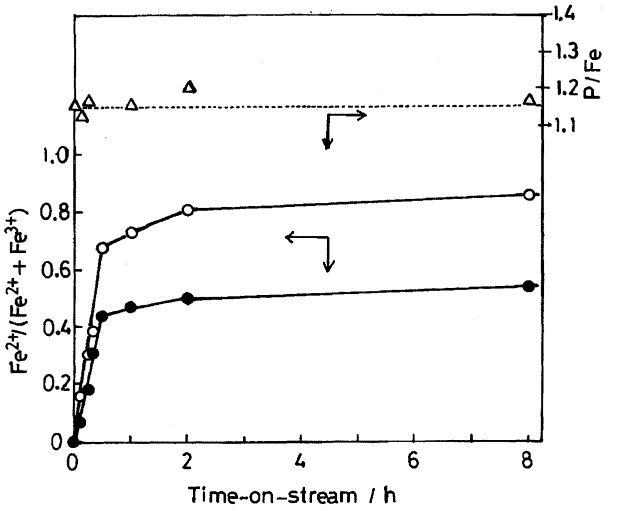

Fig. 6. Variation in P/Fe and $Fe^{2+}/(Fe^{2+}+Fe^{3+})$ ratios as a function of the reduction time. (○) in the bulk; (●) on the surface. Feed gas rates: IBA/H_2O/N_2 = 21.5/324/350 mmol h^{-1}. Sample: freshly prepared iron phosphate. Reduction temperature: 380 °C.

surface and bulk.

The spectra for Fe 2p of both fresh and used catalyst samples are shown in Fig. 4. The Fe $2p_{3/2}$ binding energy for a fresh sample [Fig. 4 (A)] was observed at 712.5 eV. This corresponds to the energy for Fe^{3+} ions without any appreciable chemical shift from standard $FePO_4$. Although the Fe $2p_{3/2}$ peak position of the used sample [Fig. 4 (B)] was close to that of the fresh sample [Fig. 4 (A)], the peak profile is slightly broader. This broadening suggests that the presence of different species from Fe^{3+} ions on the surface of the used sample.

Since the presence of Fe^{2+} ions in the bulk of used samples is known by the chemical analysis, a peak resolving for Fe^{2+} and Fe^{3+} was done by Factor analysis based on the peak profile. The dashed lines in Fig. 4 (B) show the components of Fe^{2+} and Fe^{3+}. The amounts of Fe^{2+} and Fe^{3+} species on the surface were measured by the peak areas. The values of $Fe^{2+}/(Fe^{2+}+Fe^{3+})$ ratio on the surface and in the bulk of catalyst samples are plotted as a function of the time-on-stream in Fig. 5. The values of P/Fe ratio on the surface are also shown in Fig. 5.

It was found that the $Fe^{2+}/(Fe^{2+}+Fe^{3+})$ ratios on the surface are almost the same as those in the bulk and that the P/Fe ratios on the surface are unchanged during the reaction.

On the other hand, the reaction feed gas without containing

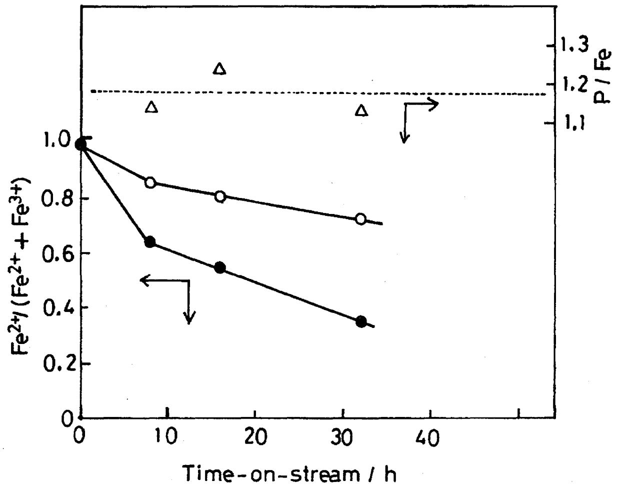

Fig. 7. Variation in P/Fe and $Fe^{2+}/(Fe^{2+}+Fe^{3+})$ ratios as a function of the time of IBA oxidation. (○) in the bulk; (●) on the surface. Sample: iron phosphate consisting of $Fe_2P_2O_7$. Reaction temperature: 380 °C.

oxygen was passed over the freshly prepared iron phosphate samples at 380 °C. The P/Fe ratio on the surface and the $Fe^{2+}/(Fe^{2+}+Fe^{3+})$ ratio on the surface and in the bulk of catalyst samples plotted as a function of the time-on-stream in Fig. 6.

The P/Fe ratio on the surface remained unchanged. The $Fe^{2+}/(Fe^{2+}+Fe^{3+})$ ratio in the bulk increased with an increase in the time-on-stream up to about 1 h and then it leveled off; after 8 h on stream, it reached about 0.9. On the other hand, the extent of increase in the $Fe^{2+}/(Fe^{2+}+Fe^{3+})$ ratio on the surface was much smaller than that in the bulk; after 8 h on stream, the ratio reached only 0.5.

The reaction was done over iron phosphate samples consisting of $Fe_2P_2O_7$ phase. The initial $Fe^{2+}/(Fe^{2+}+Fe^{3+})$ ratio in the bulk was 0.95. The P/Fe ratio on the surface and the $Fe^{2+}/(Fe^{2+}+Fe^{3+})$ ratios both on the surface and in the bulk are plotted as a function of the time-on-stream in Fig. 7. The P/Fe ratio remained unchanged during the reaction and it was the same as that in the bulk. The $Fe^{2+}/(Fe^{2+}+Fe^{3+})$ ratio on the surface decreased more rapidly than that in the bulk.

Conclusions

The new findings obtained in this study are summarized as follows.

[1] The structural changes in the bulk owing to oxidation–reduction of iron phosphates are expressed schematically as follows (Scheme 1).

[2] The structural changes in the bulk of iron phosphates during the oxidative dehydrogenation of IBA are summarized schematically as follows (Scheme 2).

[3] The catalytic performance in the oxidation of IBA is scarcely affected by changes in the structure and valence states of iron in the bulk.

[4] The P/Fe ratio on the surface is the same as that in the bulk. Further, the $Fe^{2+}/(Fe^{2+}+Fe^{3+})$ ratio on the surface varies in the same way as that in the bulk. Therefore, the catalytic actions of iron phosphate for oxidative dehydrogenation of IBA cannot be explained from the surface properties that were measured from cooled samples.

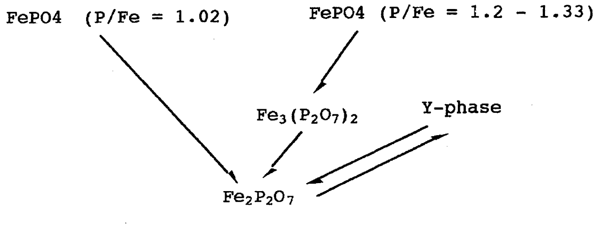

Scheme 1.

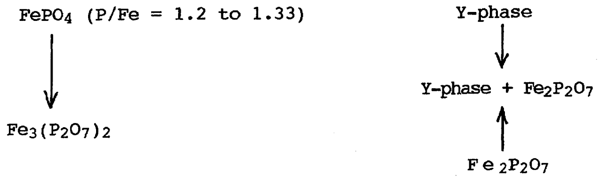

Scheme 2.

It is considered that the catalytic actions are governed by surface species that may be in equilibrium with gaseous reactants and that are too unstable to detect on the surface of cooled iron phosphate samples. Therefore, it seems necessary to measure the surface properties of samples in the working states.

References

1) A. Goiffon, J. C. Jumas, and E. Philippot, *Rev. Chim. Minér.*, **24**, 99 (1986).

2) M. Ronis and F. d'Yvoire, *C. R. Acad. Sc. Paris*, **269c**, 1388 (1969).

3) P. Von Royen and J. Korinth, *Z. Anorg. Allg. Chem.*, **291**, 227 (1976).

4) J. T. Hoggins, J. S. Swinnea, and H. Steinfink, *J. Solid State Chem.*, **47**, 278 (1983).

5) J. M. M. Millet and G. Hecquet, *Stud. Surf. Sci. Catal.*, **55**, 833 (1990).

6) M. Ijjaali, G. Venturini, R. Gerardin, B. Malaman, and C. Gleitzer, *Eur. J. Solid State Inorg. Chem.*, **28**, 983 (1991).

7) Y. Barbaux, M. Dekiouk, M. Le Mager, L. Gengembre, D. Huchette, and J. Grimblot, *Appl. Catal.*, **90**, 51 (1992).

8) M. Ai, E. Muneyana, A. Kunishige, and K. Ohdan, *J. Catal.*, **144**, 632 (1993).

9) M. Ai, E. Muneyama, A. Kunishige, and K. Ohdan, *Catal. Lett.*, **24**, 355 (1994).

10) R. A. J. Day and A. L. Underwood, "Quantitative Analysis," 4th ed, Prentice-Hall, Englewood-Cliffs, New Jersey (1980).

11) M. Ai, E. Muneyama, A. Kunishige, and K. Ohdan, *Appl. Catal. A*, **109**, 135 (1994).

12) S. Touggard, *Surf. Interface Anal.*, **11**, 453 (1988).

13) D. D. Hawn and B. M. DeKoven, *Surf. Interface Anal.*, **10**, 63 (1987).

14) P. De Volder, R. Hoogewijs, R. De Gryse, L. Fiermans, and J. Vennik, *Surf. Interface Anal.*, **17**, 363 (1991).

15) M. Ai, E. Muneyama, A. Kunishige, and K. Ohdan, *Bull. Chem. Soc. Jpn.*, **67**, 551 (1994).